# Bayesian Pot-Assembly from Fragments as Problems in Perceptual-Grouping and Geometric-Learning

The SHAPE Lab - STITCH project*
Brown University, Division of Engineering, Providence, RI 02912, USA
mailto:cooper@lems.brown.edu

## Abstract

*A heretofore unsolved problem of great archaeological importance is the automatic assembly of pots made on a wheel from the hundreds (or thousands) of sherds found at an excavation site. An approach is presented to the automatic estimation of mathematical models of such pots from 3D measurements of sherds. A Bayesian approach is formulated beginning with a description of the complete set of geometric parameters that determine the distribution of the sherd measurement data. Matching of fragments and aligning them geometrically into configurations is based on matching break-curves (curves on a pot surface separating fragments), estimated axis and profile curve pairs for individual fragments and configurations of fragments, and a number of features of groups of break-curves. Pot assembly is a bottom-up maximum likelihood performance-based search. Experiments are illustrated on pots which were broken for the purpose, and on sherds from an archaeological dig located in Petra, Jordan. The performance measure can also be an aposteriori probability, and many other types of information can be included, e.g., pot wall thickness, surface color, patterns on the surface, etc. This can also be viewed as the problem of learning a geometric object from an unorganized set of free-form fragments of the object and of clutter, or as a problem of perceptual grouping.*

Keywords: automatic pot assembly, structure from unorganized 3D data, geometric learning, perceptual grouping.

## 1 Introduction

Many archaeological excavation sites are rich in fragments of pots, called *sherds* hereafter, which are either axially symmetric,[1] or look as though they might have such rotational structure but really do not, *e.g.*, the handles of a jar or flat sections of the surface of a plate. There is great scientific and cultural interest in the archaeological community in reconstructing these axially symmetric pots from the sherds found. At present, few pots are reconstructed since the assembly is done manually and is time consuming often taking a few days for one pot. Instead, most pottery is approximately classified using two-dimensional drawing and measurement techniques [6]. This paper presents an approach to the largely automatic estimation of mathematical models of axially symmetric pots from 3D laser scanned data of the sherds. This data is a dense set of 3D points over the outer surface and perhaps other surfaces as well of each sherd, such as along breaks and the inside of the pottery.

Some work has been done on the more general problem of solving 3D puzzles via matching of either break curves [11, 5] or break surfaces [7]. Noteworthy work with respect to the specific problem of pot classification and assembly is treated by Sablatnig *et. al.* in [10]. However, none of the approaches assemble complete pots nor do they use axis/profile-curves.

## 2 Sherd Geometry Parameters

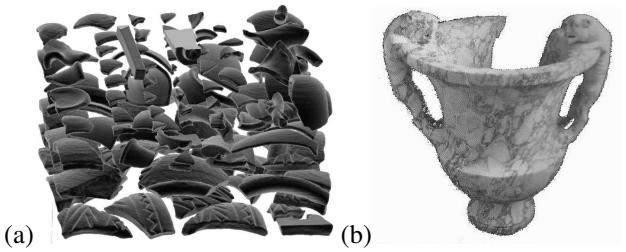

(a) (b)

Figure 1: (a) A group of sherds from a variety of pots; (b) example of an urn reconstructed from 20-30 pieces [12].

In this section we present the geometric parameters that uniquely and completely specify the geometry of a sherd or pot, indicate their role in computing the probability of

*David B. Cooper, Andrew Willis, Stuart Andrews, Jill Baker, Yan Cao, Dongjin Han, Kongbin Kang, Weixin Kong, Frederic F. Leymarie, Xavier Orriols, Senem Velipasalar, Eileen L. Vote, Martha S. Joukowsky, Benjamin B. Kimia, David H. Laidlaw, David Mumford.

[1] *I.e.*, the intersection of the pot outer surface with a plane perpendicular to the pot axis is a circle or nearly so.



from the Proceedings of ICPR (International Conference on Pattern Recognition) Vol III, August 2002

the measurement data of a group of sherds aligned as a hypothesized portion of a possible pot, and comment on the search algorithm for doing MLE or MAP estimation of a complete pot. All of these are *major new contributions* to a concept of virtual pot estimation and specific algorithms for implementing the various pieces of the approach. We assume sherds are generated as follows. Nature generates a number of pots of various shapes, breaks each pot into fragments along break curves (Fig. 2) she has drawn on the surface, scatters a subset of each such set of fragments, and also scatters some pot-like fragments that do not come from pots. Our job is to estimate mathematical models of the original pots from laser scans of these sherds found. For the purpose of this paper, we have focused on a subset of the geometric information that can be used. It consists of the outer-surface break-curves, break-curve *vertices* at T and Y junctions (Fig. 2), axis/profile curve for each aligned group, i.e. configuration, and Euclidean transformations that take each sherd from its data-measurement position to its position in a configuration. Our ultimate interest is only in estimating the axis/profile curve for a pot. The other parameters must be estimated because they explain the measurement data, but the are nuisance parameters.

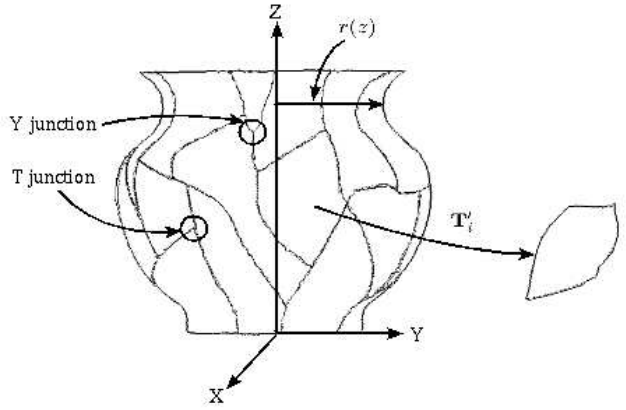


Figure 2: Geometry used ro represent a fragmented vessel.

Assume the pot is in standard position, *i.e.*, its axis is the $z$-axis and it sits on the $xy$-coordinate plane. Then the pot and its fragments are specified by vectors of parameters listed in Table 1. These are the parameters of the geometry of the fragments in their original positions. We assume that the $i^{th}$ fragment of a vessel in standard position undergoes an arbitrary Euclidean transformation, $\mathbf{T}'_i$, to move it to a measurement position, which simply consists of a rotation and translation. We call the transformed fragment a "sherd." The specific models are described later in § 3.

Sherd measurement-data is provided by a Shapegrabber laser/camera scanner [1]. It produces 15,000 3D points/sec.

| symbol | signification |
|---|---|
| $\mathbf{l}$ | $z$-axis (axis of vessel in standard position) |
| $\alpha$ | Radius curve for entire vessel (*i.e.*, profile-curve, $r(z)$, with respect to $z$-axis) |
| $\alpha_i$ | Portion of radius curve for fragment $i$ |
| $\alpha_{ij}$ | Portion for the union of fragments $i$ and $j$ |
| $\beta$ | Break-curves for entire vessel |
| $\beta_i$ | Portion of break-curves for fragment $i$ |
| $\beta_{ij}$ | Portion shared by fragments $i$ and $j$ |

Table 1: Basic geometric parameters. Note that, $\alpha$'s and $\beta$'s are all *vectors* of model parameters.

| symbol | signification |
|---|---|
| $\mathbf{U}'_i$ | Outer surface data for sherd $i$ |
| $\mathbf{V}'_i$ | Break-curve data for sherd $i$ |
| $\mathbf{V}'_{i,j}$ | Break-curve data for $i^{th}$ sherd over $i, j^{th}$ sherd break |
| $\mathbf{U}'$ | Vector composed of all the $\mathbf{U}_i$ |
| $\mathbf{V}'$ | Vector composed of all the $\mathbf{V}_i$ |

Table 2: The measurement data.

at a resolution and accuracy of the order of 0.25mm. All of these points are surface measurements, *i.e.*, measurements of outer, inner, and break surfaces including the 3D ridges that separate these surfaces. For the algorithms used in this paper, we have extracted two subsets of the measurement data: 1) those points which are measurements of a sherd outer-surface and 2) those which are measurements of a sherd outer-surface break-curve. Our approach to doing this for the data sets used in this paper is fast, based on clustering, and is described in [3].

## 2.1 Assumptions

**Surface measurement points are *iid* $\mathbf{N}(0, \sigma_s^2)$**
*These are independent, identically distributed, Gaussian perturbations perpendicular to the surface and having mean* 0 *and variance* $\sigma_s^2$. See [2] for a justification of this model.
**Break-curve measurement points are *iid* $\mathbf{N}(0, \sigma_b^2\mathbf{I})$**
*These are independent, identically distributed spherically symmetric Gaussian perturbations in 3-space about each point on the true break-curve, with mean* 0 *and variance* $\sigma_b^2$. Note that, more appropriate but more complicated models can be used.

The joint probability of all surface and break-curve data given a profile curve, a break-curve, and all transformations to sherds, can be written as:



from the Proceedings of ICPR (International Conference on Pattern Recognition) Vol III, August 2002

$$P(\mathbf{U}', \mathbf{V}'|\mathbf{T}', \alpha, \beta) = \prod_i P(\mathbf{U}'_i, \mathbf{V}'_i|\mathbf{T}'_i, \alpha, \beta). \quad (1)$$

The **MLE** is the vector of values for $\mathbf{T}', \alpha, \beta$ that maximizes (1). A combined **MAP** and **MLE** is the vector of values that maximizes $P(\mathbf{U}', \mathbf{V}'|\mathbf{T}', \alpha, \beta)P(\alpha)$, where $P(\alpha)$ is the *a priori* probability distribution for the vessel profile curve. Note that, eqn.(1) illustrates the role of $\mathbf{T}'_i$, *i.e.*, it translates $\mathbf{l}$, $\alpha_i$ and $\beta_i$ to the $i^{th}$ sherd position. Also note that estimating a virtual pot can be though of as aligning into *standard position* the data sets for the individual sherds which involves estimating $\mathbf{T}_i = (\mathbf{T}'_i)^{-1}$.

# 3 Sherd Alignment and Geometry Estimation

We begin by matching the break-curve measurements for pairs of sherds starting at their break-curve vertices. These vertices occur where two, three, and in some cases four or more, sherd corners meet. In the prevalent cases of two or three sherd vertex points, the vertices can meet in T-junctions or Y-junctions respectively (Fig. 2). Toward this end, we put down a finite number of points along the measured break-curve for each sherd starting at a vertex. Successive points are a Euclidean distance "$d$" from one another. For a given sherd, each measured break curve is matched with all the measured break curves on other sherds. The error criterion is a sum of squared errors, and the error function also contains the sum of squared differences in the measured unit normals to the surfaces at the data points used in the matches. The latter is to impose surface tangent continuity across a break curve. Let us consider the break-curve data point $\mathbf{p}_{im}$, from sherd $i$, and denote $\mathbf{R}$ and $\mathbf{t}$ as the estimated rotation matrix and translation vector coming as solution to equation (2) below, where $\lambda$ is a chosen positive constant, $\mathbf{n}_{im}$ is the unit normal to the surface data of sherd $i$ at the break-curve data-point $\mathbf{p}_{im}$ and $\mathbf{M}$ is the number of data points used, which is 5 at present. Then we have the optimization problem:

$$\min_{\mathbf{R},\,\mathbf{t}} \sum_{m=1}^{\mathbf{M}} \left[ \|\mathbf{p}_{im} - \mathbf{R}\mathbf{p}_{jm} - \mathbf{t}\|^2 + \lambda \|\mathbf{n}_{im} - \mathbf{R}\mathbf{n}_{jm}\|^2 \right]. \quad (2)$$

Equation (2) has an *explicit* solution. This is a linear least-squares problem, and the solution is computed at little cost.[2] Stored with each matched pair is the sum of squared errors between the five pairs of corresponding points used in the alignment computation. We denote this error $e_{\mathbf{T}}$:

$$e_{\mathbf{T}} \equiv \sum_{m=1}^{\mathbf{M}} \|\mathbf{p}_{im} - \mathbf{R}\mathbf{p}_{jm} - \mathbf{t}\|^2, \quad (3)$$

where $\mathbf{T}$ is the transformation that produced the best alignment. It can be shown [3] that this cost is equivalent to MLE of the common break-curve on the pot surface for the data points, $(\mathbf{p}_{im}, \mathbf{p}_{jm})$ $m = 1, \ldots, 5$. Let us assume that a sherd has 4 vertices on average, and that 200 sherds must be considered for assembly. Then, there are roughly $4 \times 200 = 800$ break-curve segments that must be compared for possible matches. Hence, there are roughly $(800^2/2) = 320,000$ pairs that must be checked for matches. If each match computation takes about one millisecond, the total of all match checks and alignments takes about 6 minutes.

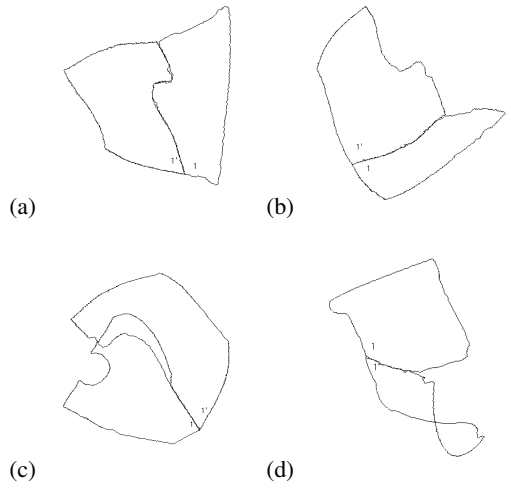


Figure 3: Break-curve pair matches.

Figure 3 shows matched and aligned break-curve data for 4 pairs of sherds. Examples (a) and (b) represent correct matches with resulting alignments. Examples (c) and (d) are incorrect matches and alignments. For the incorrect matches shown, the matching error is small, *i.e.*, the five pairs of points match well. It does occur in practice that an incorrect match may have a smaller match-error than will a correct match. Incorrect matches may be quickly identified via two methods: 1) by detecting break-curve data *overlap*, as illustrated in case (c), or 2) by comparing the *profile curve* for the surface data for each matched pair of sherds as illustrated by case (d).

An example of a correctly-matched triplet is shown in Figure 4. In these cases one sherd is held fixed and each of the other two is transformed, which means that two transformations must be estimated or 12 parameters. These parameters are estimated simultaneously using all the matching data in a single cost function. Unfortunately, in this case

[2] It takes less than a millisecond of CPU time on our PC's.

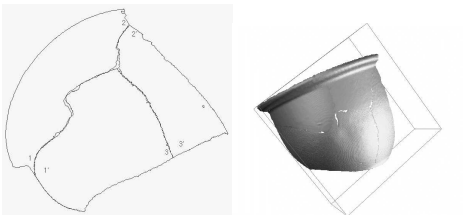

Figure 4: Example of a break-curve triplet match.

the estimation is *nonlinear*. The approach extends immediately to four or more groups of sherds, where $k-1$ transformations must be estimated simultaneously for optimally matching $k$ sherds.

Whereas effective algorithms have been developed for estimating the axis and associated profile curve for a sherd that comprises a large portion of the surface of an axially symmetric pot, there do not appear to be effective algorithms for estimating a pot axis when the sherd is a *very small portion of the pot* or when the *profile curve is complicated*. But these cases are important in practice and challenging in concept. We consider two approaches to estimating axis/profile-curves: one makes use of spheres of curvature and the other uses algebraic surface models.

(a) p1135 (b) p654 (c) p1313

Figure 5: A spectrum of archaeological sherds from the Great Temple site of Petra, Jordan [4], used to illustrate our axis/profile-curve estimation.

We have parameterized the axis of symmetry, $\mathbf{l}'$, using the standard parametric equation of a 3D line:

$$\begin{aligned} x &= m_x z + b_x \,, \\ y &= m_y z + b_y \,. \end{aligned} \tag{4}$$

These equations contain four unknown parameters. Two of these, $m_x$ and $m_y$, describe the slope of the line when it is projected onto the $xz$-plane and the $yz$-plane, respectively. The remaining two parameters, $b_x$ and $b_y$, specify where the line intercepts the $xy$-plane at $z = 0$.

The first method uses an algebraic surface model [9] (equivalently, an algebraic profile-curve model) and can handle shapes for which the radius function is multivalued (Fig. 6a). An algebraic curve of degree $d$ has $[(d+1)(d+2)/2]$ unknown coefficients and takes the following form:

$$f_d(r,z) = \sum_{0 \le j+k \le d;\ j,k \ge 0} a_{jk} r^j z^k = 0 \,. \tag{5}$$

Here, $d$ is a parameter which is related to the geometric complexity of the pottery sherd profile-curve to be estimated. For the artifacts in this paper, all experiments are performed with $d = 6$. These and the axis parameters define the objective function (6) below, which is a modified version of the energy function in [9], for estimating the profile curve coefficients:

$$e_{grad} = \sum_{i=1}^{I} \left( f_d^2(r_i,\, z_i) + \mu \ \left\| \mathbf{n}_i^p - \nabla f_d(r_i,\, z_i) \right\|^2 \right), \tag{6}$$

Since the surface model depends on the axis, the resulting objective function is highly non-linear. Consequently, convergence to a local minimum may occur if minimization is started far from the true parameter value. The estimation algorithm needs only a hypothesized axis of symmetry in order to begin. In practice, we begin with the axis estimate provided by an improved version of the Plücker coordinates method as described in [8]. This initial estimate is very fast — probably less than a millisecond. The total computation time[3] is of the order of 1 to 3 minutes for roughly 3,000 data points.

Figure 5 shows a set of three sherds from an archaeological dig at Petra, Jordan [4], which were used to illustrate the algorithm above. The sherd surface-data is overlaid in white on the estimated pot-surface. Also, upon rotating the estimated sherd data-axis to coincide with the $z$-axis, the distance of each 3D surface data-point is plotted as a function of $z$. The narrowness of the swaths of data in Figure 6 demonstrate the accuracy of our estimates for axes for these difficult examples. 5.(a) is an example of a small sherd having a somewhat complicated multi-valued radius function $r(z)$. Note from Figure 5.(b) that accurate estimates may be derived from sherds which seem to contain little shape information. Figure 5.(c) gives a good appreciation of how much information may be extracted from a large piece.

Using the second method, we define *spheres of curvature* which are the spheres centered at one of the principal centers of curvature and having radius equal to the corresponding radius of curvature. These spheres are tangent to the surface. It is easy to show that for each point on the surface, the center of the sphere of principal curvature corresponding to the parallel circles is on the main axis (of revolution).

[3] Implemented using the C programming language.

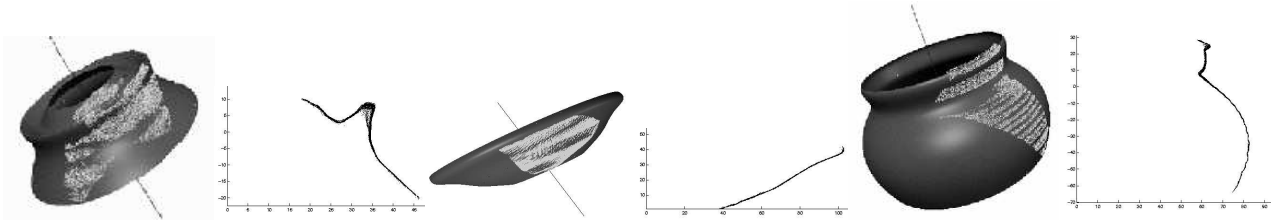

(a) p1135 (b) p654 (c) p1313

Figure 6: Axis/profile-curve estimates for the sherds of Figure 5, and their estimated 3D pot models.

By finding the line which minimizes the least squares distance from the estimated centers to a hypothesized axis, we can estimate the main axis and then its profile curve.

One useful feature of a surface of revolution is that the principal curvature corresponding to the parallel circles does not depend on second derivatives; our approach is therefore more robust to noisy data. We denote this principal curvature $\kappa_\pi$. Given a set of $m$ 3D data-points from a surface of revolution, let $\mathbf{p}_i$ and $\mathbf{n}_i$ be the $m$ 3D data points and their corresponding normals. Suppose the axis of revolution is the line $\mathbf{l}$. This axis can be specified by a point $\mathbf{p}_0$ on $\mathbf{l}$ and a unit vector $\mathbf{w}$ corresponding to the direction of $\mathbf{l}$. We make the point $\mathbf{p}_0$ unique by requiring $\mathbf{p}_0 \cdot \mathbf{w} = 0$. For any point $\mathbf{p}$ on the surface, suppose the normal at that point is $\mathbf{n}$. It can be shown that

$$\kappa_\pi = \frac{\|\mathbf{n} \times \mathbf{w}\|}{\|(\mathbf{p} - \mathbf{p}_0) \times \mathbf{w}\|} .$$

All the centers of the sphere of curvature corresponding to $\kappa_\pi$ should be on the axis of revolution, hence we can minimize following function:

$$f(\mathbf{p}_0, \mathbf{w}) = \sum_{i=1}^{m} \left\| (\mathbf{p}_i - \mathbf{p}_0) \times \mathbf{w} - \frac{\|(\mathbf{p}-\mathbf{p}_0)\times\mathbf{w}\|}{\|\mathbf{n}\times\mathbf{w}\|}(\mathbf{n}_i \times \mathbf{w}) \right\|^2 .$$

There are six parameters in the function $f$, which are not independent. They satisfy the following constraints:

$$\mathbf{p}_0 \cdot \mathbf{w} = 0 \ \text{ and } \ \|\mathbf{w}\| = 1 .$$

We want to reduce the six dependent parameters to four independent parameters. Define the matrix $R$ as following:

$$R = \begin{bmatrix} \cos\phi\sin\psi & \sin\phi\cos\psi & \sin\psi \\ -\sin\phi & \cos\phi & 0 \end{bmatrix} ,$$

then the vector $\mathbf{w}$ can be represented as:

$$\mathbf{w} = \begin{bmatrix} -\cos\phi\sin\psi & -\sin\phi\sin\psi & \cos\psi \end{bmatrix}^T .$$

Define $\mathbf{p}'_0 = (x'_0, y'_0)^T = R \cdot \mathbf{p}_0$. Then the objective function $f$ can be represented as a function of four parameters, $\phi, \psi, x'_0, y'_0$:

$$f(\phi, \psi, x'_0, y'_0) = \sum_{i=1}^{m} \left\| (R \cdot \mathbf{p}_i - \mathbf{p}'_0) - \frac{\|(R\cdot\mathbf{p}-\mathbf{p}'_0)\|}{\|R\cdot\mathbf{n}_i\|}(R \cdot \mathbf{n}_i) \right\|^2 . \quad (7)$$

Weighted least squares takes care of outliers. The objective function 7 is easy to calculate, and the minimization can be carried out by general iterative methods, beginning with the Plücker coordinates method described in [8]. In its present implementation, the computation time is a few minutes in MATLAB® for a dataset of a few thousand points.

# 4 Sherd Joint-Geometry Estimation

During pot assembly, sherds are assembled into *configurations*, each configuration is an assembly of a subset of sherds aligned based on their break-curve and associated surface data. In this section we treat the problem of estimating the joint geometry of an arbitrary number of sherds based on the preceding measurement data alone. The sherd surface and boundary parameters obtained via methods in § 3 are combined into a single cost function which is a sum of the cost functions previously mentioned.

Denote (all) the available geometric data by $\Theta_{i,j}$, the break-curve data by $\Phi_{i,j}$ and the surface data by $\Omega_{i,j}$, this for sherds $i$ and $j$. Then alignment and pot model estimation for sherd $i$ and $j$ data sets jointly, is done by the minimization over all geometric parameters, *i.e.*:

$$\begin{aligned} \min\left[-\log P\left\{\Theta_{i,j} \mid \beta_{ij}, \mathbf{l}_{ij}, \mathbf{T}_{ij}, \alpha_{ij}\right\}\right] &= \\ \min\left[-\log P\left\{\Phi_{i,j} \mid \mathbf{T}_{ij}\right\} - \log P\left\{\Omega_{i,j} \mid \mathbf{T}_{ij}, \mathbf{l}_{ij}, \alpha_{ij}\right\}\right] &= \\ e_{\mathbf{T}} + e_{grad} + \text{constant} , & \end{aligned}$$

where the two energies, $e_{\mathbf{T}}$ and $e_{grad}$, are defined in equations (3) and (6), respectively.

The implemented algorithm uses approximations for doing the minimization, is computationally fast, and is reasonably accurate for the few examples tried. Figure 7 shows results for one such experiment. This algorithm is presently undergoing refinement to speed it up considerably.

# 5 Pot Assembly Search Algorithm

The sherds may only describe a single or several small portions of the overall vessel. Therefore, the pot assembly algorithm must accomodate for situations where the input data may be missing data for some pieces or include groups of pieces which may belong to entirely different vessels.

To this end, we propose a MLE-based algorithmic search in order to robustly perform pot assembly. The algorithm examines *significant* joint-geometries of various sherd groups according to the method described in § 4. Here and afterwards *significant* denotes those configurations whose joint-geometry *cost* (cost is the negative of the loglikelihood) represents a possible (i.e. not-improbable) solution. At the moment, we are considering typical datasets which consist of 100 to 200 sherds, which, as indicated, could come from a number of pots as well as from other objects. We proceed as follows:

1. Estimate the axis/profile-curve for each of the sherds §3 (*Computationally costly*).

2. For each pair of sherds, estimate all reasonable alignments using break-curve data §3 (*Computationally fast*).

3. For each significant configuration, improve the alignment using § 4 and store configurations and individual sherds in order of increasing cost in a stack (*Computationally of medium cost at present*).

4. Starting with the top item in the stack, go down through the stack and merge the configuration with those lower in the stack that result in roughly lowest cost configurations according to § 4. Update the stack. Note, a sherd can appear only once in a configuration, though the same sherd can appear in many configurations. Return to step 3 or stop (*Computationally of medium cost at present*).

Note, this search proceeds along contours of constant configuration-probability to find the most probable virtual pot. Hence realizations of high probability will perpetuate through the search algorithm whereas improbable geometries will eventually not be considered.

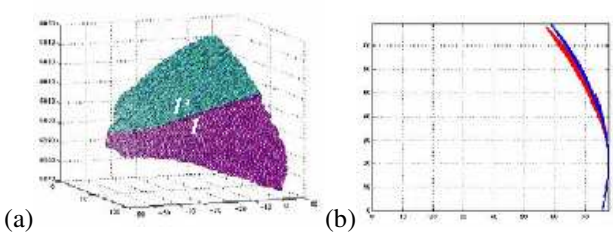


Figure 7: Estimated joint geometry. The two sherd data sets fit together well, (a); the projected-data scatter about the estimated profile curve is small, (b).

# 6 Conclusion

A Bayesian approach has been outlined for the estimation of mathematical representations for pots based on sherds found at archaeology sites. The key algorithms for implementing the approach have been developed, and experimental results from these algorithms to real sherd 3D data have been presented and discussed. At this time, experiments have been run on automatic matching and aligning pairs and triples of sherds.

The framework discussed in this paper is for estimating arbitrary *a priori* unknown axially-symmetric pot models. Hence, it is *unsupervised* pot geometry-learning from sherd data. If instead we know *a priori* that the pot sherds present are not arbitrary but rather that each belongs to one of a group of 10 known pot shapes, the problem is computationally much easier because the sherd alignment problem is then more of a pot shape-recognition problem and less of a shape-estimation problem.

The framework presented can accommodate additional geometric and pattern information which should result in doing the pot estimation faster, or with fewer sherds, or estimating models for more complex objects.

The axis/profile-curve estimators can be thought of as generalized cylinder axis/cross-section estimators, and are more accurate for these small data fragments than any algorithms demonstrated to date.

# References

[1] Shapegrabber inc. http://www.shapegrabber.com.

[2] R. Bolle and D. B. Cooper. On optimally combining pieces of information, with application to estimating 3-D complex-object position from range data. *IEEE Trans. on Pattern Anal. Machine Intell.*, 8(5):619–638, September 1986.

[3] D. Cooper, A. Willis, Y. Cao, D. Han, F. Leymarie, X. Orriols, D. Mumford, et al. Assembling virtual pots from 3D measurements of their fragments. In *VAST International Symposium on Virtual Reality Archaeology and Cultural Heritage*, 2001.

[4] M. S. Joukowsky. *Petra Great Temple - Volume 1: Brown University Excavations 1993-1997*. Petra Exploration Fund, Providence, RI, USA, 1999. 390 pages.

[5] W. Kong and B. B. Kimia. On solving 2D and 3D puzzles using curve matching. In *Proc. of CVPR*, Hawaii, USA, December 2001. IEEE, Computer Society.

[6] V. Nautiyal, S. Nautiyal, and M. Naithani. Optical plotting and AutoCAD for drawing pottery. *CSA Newsletter*, XII(3), Winter 2000. www.csanet.org/newsletter/winter00/nlw0003.html.

[7] G. Papaioannou, E.-A. Karabassi, and T. Theoharis. Virtual archaeologist: Assembling the past. *IEEE Computer Graphics and Applications*, 21(2):53–59, March/April 2001.

[8] H. Pottmann, M. Peternell, and B. Ravani. An introduction to line geometry with applications. *Computer-Aided Design*, 31:3–16, 1999.

[9] T. Tasdizen, J. P. Tarel, and D. B. Cooper. Improving the stability of algebraic curves for applications. *IEEE Trans. on Image Proc.*, 9(3):405–416, March 2000.

[10] S. Tosovic and R. Sablatnig. 3D modeling of archaeological vessels using shape from silhouette. In *Third International Conference on 3D Digital Imaging and Modeling*, Quebec, Canada, June 2001.

[11] G. Ucoluk and I. H. Toroslu. Automatic reconstruction of broken 3-D surface objects. *Comp. and Graph.*, 23(4):573–582, Aug. 1999.

[12] T. Weber and R. Wenning. *Petra*. Verlag Phillip Von Zabern, Germany, 1997.